Title: White matter changes in focal to bilateral tonic-clonic seizures

Authors: Christina Maher[1,2,3], Arkiev D'Souza[2,4], Rui Zeng[5], Michael Barnett[5,6,7], Omid Kavehei[1,3], Armin Nikpour[8], Chenyu Wang[5,7]

1. The University of Sydney, School of Biomedical Engineering, Faculty of Engineering, Sydney, Australia; 2. The University of Sydney, Brain and Mind Centre, Sydney, Australia; 3. The University of Sydney, Australian Research Council Training Centre for Innovative BioEngineering, Sydney, Australia; 4. The University of Sydney, Central Clinical School, Faculty of Medicine and Health, Sydney, Australia; 5. The University of Sydney, Brain and Mind Centre - Translational Research Collective, Faculty of Medicine and Health, Sydney, Australia; 6. Sydney Neurology, Camperdown, Australia; 7. Sydney Neuroimaging Analysis Centre, Camperdown, Australia; 8. Royal Prince Alfred Hospital, Comprehensive Epilepsy Service and Department of Neurology, Camperdown, Australia

Abstract

Objective: A better understanding of the mechanistic underpinnings of focal to bilateral tonic-clonic seizures (FBTCS) would aid treatment decisions, and improve disease management for drug-refractory patients. We sought to examine the microstructural white matter differences in patients with FBTCS, compared to those with focal epilepsy without FBTCS, and control participants.

Methods: We combined a superior tract segmentation model with track-weighted tensor metrics (TW-TM) in an advanced, automated image analysis and tract reconstruction pipeline. Univariate analysis of covariance (ANCOVA) tests were used to compare group differences in both whole-tract metrics and hemispheric tract metrics.

Results: We identified a range of white matter regions that displayed significantly altered white matter in patients with and without FBTCS, compared to controls. Specifically, patients without FBTCS had significantly increased white matter disruption in the inferior fronto-occipital fascicle and the striato-occipital tract. In contrast, patients with FBTCS were more similar to healthy controls in most regions, except for distinct alterations in the inferior cerebellar region compared to the non-FBTCS group and controls.

Significance: To our knowledge, this is one of few studies to exploit track-weighted tensor metrics (TW-TM) to investigate white matter changes in FBTCS. Our study reveals marked

alterations in a range of subcortical regions widely considered critical in the genesis of seizures. Our application of TW-TM in a new clinical dataset allowed the identification of specific tracts that may act as a predictive biomarker to distinguish patients who are likely to develop FBTCS.

Keywords: "Focal epilepsy", "Focal to bilateral tonic-clonic seizure", "diffusion tensor imaging", "tractography", "white matter".

Key points:

- We compared white matter alterations in 25 patients with and without focal to bilateral tonic-clonic seizures (FBTCS) to 19 controls.
- Track-weighted tensor-metrics (TW-TM) revealed the FBTCS group had distinct alterations in the inferior cerebellar region.
- Increased WM disruption was observed in the inferior-fronto-occipital and striato-occipital tracts in the non-FBTCS group.
- The TW-TM showed increased white matter disruption in the inferior-fronto-occipital and striato-occipital tracts in the non-FBTCS group.
- Results suggest certain subcortical white matter alterations may inhibit FBTCS, further research is needed to validate these observations.

1 INTRODUCTION

For drug-resistant patients with focal to bilateral tonic-clonic seizures (FBTCS), there is an increased risk of cardiac arrhythmias[1], seizure-related injuries[2] and sudden unexpected death in epilepsy (SUDEP)[3]. Unlike other epilepsies, such as temporal lobe epilepsy (TLE), where the role of structural regions is largely understood, the mechanisms underlying FBCTS remain elusive. Therefore, the importance of delineating the mechanisms involved in FBTCS is amplified as a vital objective to aid control of FBTCS and prevention of SUDEP.

Although the taxonomy of FBTCS implies whole-brain generalisation of seizures, FBTCS are primarily highly selective, producing more vigorous activity in specific brain regions[4,5]. Mounting evidence has endorsed the subcortical structures such as the thalamus and basal ganglia (BG) and their associated circuits as critical to the information relay involved in

FBTCS. The thalamocortical relay fibres are topographically arranged to project to the cerebral cortex, from which sensory information is processed and relayed back to the original projection site in the thalamus. Acting as a "relay station"[6], the thalamus has widespread connections across the entire cerebral cortex and moderates communication between various brain regions. Within the context of FBTCS, the thalamus has been proposed as a support system for seizure propagation via its role in the synchronisation of abnormal cortical-subcortical ictal discharge[7,8].

On the other hand, the BG functions as a "braking system", interacting with the thalamus and cortex through multiple parallel circuits, including the direct and indirect pathways[9]. The BG is increasingly hypothesised to play an anticonvulsive role in FBTCS[10], yet specific mechanisms remain unclear. Increased BG activity was reported to be negatively associated with FBTCS in TLE[11,12]. In contrast, others illustrated that the BG only become involved when ictal activity disperses to additional cortical regions during secondary generalisation[13].

The subcortical structures involved in FBTCS are also involved in focal seizures[14]. We included both patient groups (focal and focal with FBTCS) in this study to address the distinct structural differences between the two groups. In addition to the thalamic and striatal regions, we included other white matter regions based on their well-documented role in focal seizures and functional connectivity[15], to determine whether any observed group differences were unique to the FBTCS group, and to account for possible whole brain differences.

Tensor-based metrics derived from diffusion tensor imaging (DTI) have been used to identify microstructural white matter alterations in a range of epilepsies[16]. Meta-analysis showed patients with focal epilepsy had elevated regional mean diffusivity relative to controls[16]. However, FA findings are less consistent; some studies report reduced FA in patients with epilepsy compared to controls[17], whilst others report no change across various regions[18,19]; thus, further clarification is required. Moreover, though tensor-based metrics have been established as a valuable technique to elucidate the mechanisms of focal epilepsy, they are seldom applied to FBTCS.

This study measured tensor-based metrics to explore new biomarkers in patients with focal epilepsy and FBTCS. We hypothesised that compared to controls, (1) patients with focal epilepsy would have significantly altered white matter in a range of subcortical regions; (2) the patients with FBTCS would have significantly altered white matter in the thalamic and striatal regions compared to those without FBTCS.

2 METHODS

2.1 Participants and Data

Twenty-seven adults with focal epilepsy were recruited from the Comprehensive Epilepsy Centre at the Royal Prince Alfred Hospital (Sydney, Australia); and MRI was performed at the Brain and Mind Centre (Sydney, Australia). Inclusion criteria were adults diagnosed with focal epilepsy, aged 18-60, presenting without surgery, and with or without a cortical brain lesion, who were willing and able to comply with the study procedures for the duration of their participation. Exclusion criteria were pregnant women and individuals with intellectual disabilities. The 20 healthy controls (5M, 15F, mean age 37±11.12 years) were neurologically normal individuals. Written informed consent was obtained from all participants before study participation. The ethics committee of the Sydney Local Health District (SLHD) Royal Prince Alfred Hospital (RPAH) gave ethical approval (ID: X14-0347; & HREC/14/RPAH/467).

2.1.1 Epilepsy patient groups

The participants with focal epilepsy were placed into the following groups:

1. "All patients": The entire cohort of patients; all diagnosed with focal epilepsy.
2. "FBTCS-Y": In this subgroup, patients were defined as having frequent (more than two per year) or infrequent (one per year) large, homolateral and simultaneous FBTCS. The FBTCS may have occurred during observation at the RPAH Epilepsy Centre or reported by the participant as occurring elsewhere.
3. "FBTCS-N": In this subgroup, patients had never experienced a FBTCS.

2.2 Image acquisition

All scans were acquired on the same GE Discovery™ MR750 3T scanner (GE Medical Systems, Milwaukee, WI). For each participant, the following MRI sequences were acquired:

Pre-contrast 3D high-resolution T1-weighted image (0.7mm isotropic) using fast spoiled gradient echo (SPGR) with magnetisation-prepared inversion recovery pulse (TE/TI/TR=2.8/900/7.1ms, flip angle=12); and axial diffusion-weighted imaging (2mm isotropic, TE/TR=85/8325ms) with a uniform gradient loading (=1000s/mm^2) in 64 directions and 2 b 0 s . An additional b 0 image with reversed phase-encoding was also acquired for distortion correction[20]. A schematic of the image analysis pipeline is shown in Figure 1.

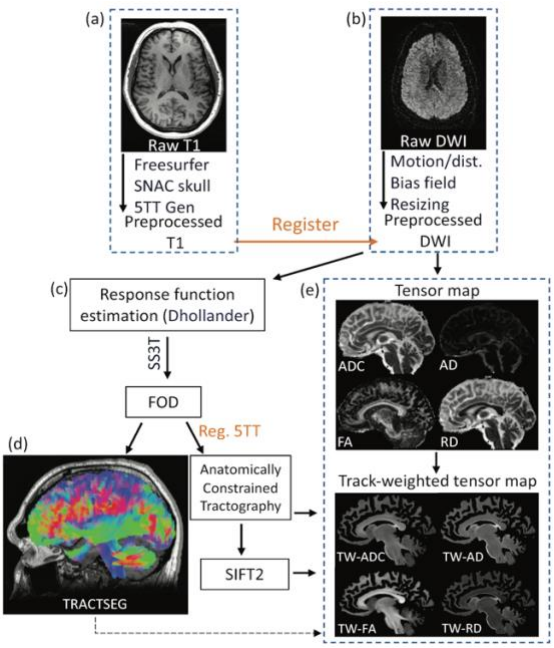

Figure 1. Schematic overview of imaging analysis pipeline. T1 (a) and diffusion MRIs (b) were preprocessed as described in Methods section 2.3. Next, further diffusion image processing and tractography was conducted (c) and tract segmentation performed (d). Finally, track-weighted tensor maps were produced, and the resulting metrics were derived (e).

2.3 Image preprocessing

The T1 images (shown in Fig. 1.a) were processed using a modified version of Freesurfer's recon-all (v6.0)[21], alongside an in-house skull-stripping tool (Sydney Neuroimaging Analysis Centre). Each subject was inspected, and minor segmentation errors were manually corrected. A 5-tissue-type (5TT) image was generated using MRtrix3[22]. The T1 image was registered to the mean b0 image; the warp was used to register the 5TT image to the diffusion image.

Diffusion image processing (in Fig. 1.b) was conducted using MRtrix3[22]. The diffusion pre-processing included motion and distortion correction[20,23], bias correction using ANTS[24], and resizing to voxel size 1 mm isotropic. The *dhollander* algorithm[25] (Fig. 1.c) was used to estimate the response functions of the white matter, grey matter, and cerebral spinal fluid, from which constrained spherical deconvolution was used to estimate the fibre orientation distributions using MRtrix3Tissue[22]. The intensity of the white matter fibre orientation distributions was normalised[22], and used for anatomically constrained whole-brain tractography[26]. The tractography settings were: 15 million tracks were generated, iFOD2 probabilistic fibre tracking[27], dynamic seeding[28], maximum length 300 mm, backtrack selected and crop at grey-matter-white-matter interface selected. For quantitative analysis, the corresponding weight for each streamline in the tractogram was derived using SIFT2[28] (Fig. 1.c); the streamline weights and tractogram were used to generate a track-density image (TDI)[29].

Track-weighted tensor-based measurements The pre-processed diffusion image was used to calculate the diffusion tensor. By resolving the tensor into its primary, secondary and tertiary directions of diffusion, the following tensor-based metrics can be calculated: apparent diffusion coefficient (ADC, the average of the three directions of diffusion), fractional anisotropy (FA, degree of anisotropy ranging from 0 to 1, whereby 0 indicates isotropic diffusion and 1 indicates diffusion exclusively along a single axis), axial diffusivity (AD, the primary direction of diffusion, representative of diffusion parallel to axonal fibres) and radial diffusivity (RD, the average of the secondary and tertiary directions of diffusion, representing diffusion perpendicular to axonal fibres)[30]. The tensor metrics (ADC, FA, AD, and RD) were estimated from the tensor maps (Fig. 1.e). Next, the tracks (and their weights) were used to calculate the track-weighted (TW) tensor-based maps and the resulting metrics (i.e., TW-ADC, TW-FA, TW-AD, TW-RD, shown in Fig. 1.e)[31], known to improve reproducibility and variability (compared to standalone tensor-based metrics)[32]. The following settings were used to generate TW images: Gaussian statistic, full-width-half-maximum of 40 and voxel size of 0.2mm.

Measuring tract-specific, track-weighted tensor-based metrics Tractseg[33], a superior automated tract segmentation model, was applied to the resized diffusion images to obtain data-driven, subject-specific segmentations of the selected tracts (illustrated in Fig. 1.d). The tracts of interest were: Thalamus - Prefrontal (TPREF), Premotor (TPREM), Precentral (TPREC), Postcentral (TPOSTC), Parietal (TPAR), and Occipital (TOCC); Striato - Fronto-Orbital (STFO), Prefrontal (STPREF), Premotor (STPREM), Precentral (STPREC), Postcentral (STPOSTC), Parietal (STPAR), and Occipital (STOCC); Anterior thalamic radiation (ATR), Superior thalamic radiation (STR), Corticospinal (CST), Fronto pontine (FPT), Parieto-occipital pontine (POPT), Inferior cerebellar peduncle (ICP), Middle cerebellar peduncle (MCP), Superior cerebellar peduncle (SCP), Inferior fronto-occipital fascicle (IFO), Uncinate fascicle (UF), Commissure anterior (CA), and Corpus callosum (CC). Two brain imaging specialists (CW and AD) conducted a quality control check by visually inspecting each tract for consistency and anatomical correctness. The right TPAR tract failed the quality control check in 10 participants; therefore, the whole tract was removed from the analysis. Twenty-four tracts were included in the final statistical analysis.

2.4 Statistical analysis

Demographics The chi-square test was used to investigate the following associations: lesion presence and drug resistance; lesion presence and seizure onset side; and lesion presence and FBTCS. Pearson correlation tested gender and age differences between groups and the association between seizure onset age and disease duration.

Group comparisons: All patients versus controls To examine whole-tract differences between groups, the weighted average of the left and right side of each tract was calculated using the equation [WeightedAverage-TW-TM = $((L_{\text{TW–TM}} \times L_{\text{count}}) + (R_{\text{TW–TM}} \times R_{\text{count}}))/(L_{\text{count}} + R_{\text{count}})$] (TW-TM: track-weighted tensor metric i.e. TW-ADC; count: tract count). Univariate analysis of covariance (ANCOVA) tests were used to examine the whole-tract differences for each TW-TM (i.e., TW-ADC, TW-FA) between "all patients" and control participants. A separate set of ANCOVAs was employed to investigate group differences in TW-TM in a given hemisphere. Here, the tract measurement from a given hemisphere was compared between all patients withepilepsy and control participants.

Group comparisons: FBTCS-Y, FBTCS-N versus Controls Another set of univariate ANCOVAs were used to investigate differences between the patient subgroups (FBTCS-Y, FBTCS-N) and control participants. Again, the weighted average of each tract's left and right sides was computed (as described above) to investigate whole-tract differences in TW-TM between the three groups. A separate set of ANCOVAs was used to investigate group differences in a given hemisphere. Here, the tract measurement from a given side was compared between the three groups.

To account for age effects on diffusivity, age was included as a covariate in all the ANCOVAs[34]. The threshold for statistical significance was set at $p = 0.05$; the Bonferroni adjusted means (which correct for multiple comparisons) were selected for the pairwise comparisons. All statistical analyses were conducted in SPSS v28.

3 RESULTS

3.1 Demographics

Twenty-five patients (10M, 15F, mean age 40±12.7 years, 17 with FBTCS-Y and 8 with FBTCS-N) and 19 controls were included in this study after passing the imaging quality control check. There were no significant differences in age or gender in both grouping conditions ("all patients" versus controls; and FBTCS-Y, FBTCS-N versus controls). There was no significant association between lesion presence and seizure onset zone; or lesion presence and FBTCS. The characteristics of patients and controls are shown in Table 1.

3.2 All patients versus controls

Group differences were tested using ANCOVAs in the two grouping conditions ("all patients" versus controls; FBTCS-Y and FBTCS-N versus controls). The whole-tract, average TW-ADC was higher in the "all patients" group compared to controls, for 16 out of 24 tracts ($p < 0.05$). The UF tracts had a lower average TW-FA in the "all patients" group compared to controls ($p < 0.05$). Nineteen tracts had higher average TW-RD in the "all patients" group compared to controls ($p < 0.05$). The MCP and SCP had higher average TW-AD in "all patients" compared to controls ($p < 0.05$). All mean differences, p values and confidence intervals are shown in Supplementary Table 1.

Table 1. Characteristics of patients and controls.

	FBTCS-Y (19)	FBTCS-N (8)	HC (20)	Description
Age* (M ±SD)	38 ±11.15	46 ±15.21	37 ±11.12	
Gender (M / F)	8 / 11	3 / 5	5 / 15	
Onset side (L / R / U)	8 / 9 / 2	3 / 3 / 2	NA	
Onset Age (M ±SD)	18 ±14.36	30 ±20.96	NA	
Disease duration (M ±SD)	27 ±16.14	22 ±12.31	NA	
Drug resistant (Y / N)	14 / 5	4 / 4	NA	
Auras	11	7	NA	
Handedness (L / R / U)	3 / 15 / A	1 / 4 / 3	NA	
MRI findings	11	4	NA	Normal
	4	1	NA	MCD
	2	1	NA	CD/FCD
	1 (R)	1 (L)	NA	Hippocampal cyst
	1	1	NA	Various (i.e. PVH, DNET)
Epilepsy classification	2 / 2	0	NA	Frontal (L / R)
	1 / 2	0	NA	Temporal (L / R)
	1 / 1	2 (R)	NA	Parietal (L / R)
	1 / 1	1 (L)	NA	Occipital (L / R)
	3 / 2	1 / 1 / 1 (U)	NA	Frontotemporal (L / R)
	1 (L)	1 (L)	NA	Frontocentral (L / R)
	2	1	NA	Unknown

Key: L: left, R: right, U: unknown, * age at the time of MRI scan, A: ambidextrous, CD: cortical dysplasia, DNET: dysembryoplastic neuroepithelial tumour, FCD: focal cortical dysplasia, MCD: malformations of cortical development, PVH: periventricular heterotopia. Two patients and one control participant did not pass the imaging quality control check and were removed from the study.

When investigating the group differences between tract sides, the "all patients" group had a higher average TW-ADC than the controls for 13 left tracts and 14 right tracts ($p < 0.05$). In the right UF tract, the average TW-FA was lower in "all patients" compared to controls ($p < 0.05$). Different to the whole-tract TW-FA results, the left TPREC and right ATR tracts had lower average TW-FA in the "all patients" group compared to controls ($p < 0.05$). The average TW-RD was higher in "all patients" compared to controls ($p < 0.05$) for all tracts across both sides except for the following: the left ICP, SCP, STFO, and STOCC tracts; the right CST, POPT, ICP, SCP, STOCC, STPAR, STPOSTC, and TPOSTC tracts. The average TW-AD was higher in "all patients" compared to controls in both sides of the

SCP and in the right TOCC tract ($p < 0.05$). All mean differences, p values, and confidence intervals are shown in Supplementary Table 2.

3.3 FBTCS-Y, FBTCS-N versus Controls

Group differences were observed in the whole-tract, average TW-ADC for 18 out of 24 tracts ($p < 0.05$). The post hoc tests revealed that the FBTCS-N group had higher TW-ADC in 17 tracts (excluding the STPOSTC) compared to controls ($p < 0.05$). The FBTCS-N group also had higher TW-ADC than the FBTCS-Y group in the IFO, STOCC, and TOCC tracts ($p < 0.05$). Group differences in the average TW-FA were observed in the CC and TPREM tracts. Post hoc tests showed that in both tracts, the FBTCS-N group had lower TW-FA than controls ($p < 0.05$). Group differences in the average TW-RD were observed for 20 out of 24 tracts ($p < 0.05$). Post hoc tests showed that in all 20 tracts, the FBTCS-N group had higher TW-RD than controls ($p < 0.05$). Group differences in the average TW-AD were observed in the MCP, IFO, STOCC and TOCC tracts. Post hoc tests showed that in the IFO and STOCC tract, the FBTCS-N patient group had higher TW-AD than the FBTCS-Y group ($p < 0.05$); and higher TW-AD than controls in all four tracts. In addition, the FBTCS-Y group had higher TW-AD than controls in the MCP ($p < 0.05$). All mean differences, p values, confidence intervals and main effects are shown in Supplementary Table 3.

When investigating group differences between tract sides, group differences were observed in the average TW-ADC of 17 left and 14 right tracts ($p < 0.05$). Post hoc tests showed that on both sides, the FBTCS-N group had higher TW-ADC than controls for all tracts ($p < 0.05$). Additionally, the FBTCS-N group had higher TW-ADC than FBTCS-Y in the right IFO ($p < 0.05$). Group differences were observed in the average TW-FA of the following right tracts: ATR, FPT, SCP, TPREF, TPREM and UF ($p < 0.05$). Post hoc tests showed that the FBTCS-N group had lower TW-FA than controls in the FPT, TPREF and TPREM tracts ($p < 0.05$). In addition, the FBTCS-N group had a lower TW-FA than the FBTCS-Y group in the SCP, and the FBTCS-Y group had lower TW-FA than controls in the UF ($p < 0.05$). Group differences were observed in the average TW-RD of 18 left and 16 right side tracts ($p < 0.05$). Post hoc tests showed that the FBTCS-N group had higher TW-RD than controls for all tracts ($p < 0.05$) except for the UF and STPREC tract. Group differences were observed in the average TW-AD of the right IFO, STOCC, and TOCC

tracts ($p < 0.05$). Post hoc tests revealed that the FBTCS-N group had higher TW-AD than controls in all three tracts ($p < 0.05$) and higher TW-AD than the FBTCS-Y group in the IFO ($p < 0.05$). All mean differences, p values, confidence intervals and main effects are shown in Supplementary Table 4.

4 DISCUSSION

Distinct from previous works, this study implemented an automated, track-weighted tensor imaging pipeline to examine the microstructural white matter changes in patients with and without FBTCS compared to controls. Our study revealed unexpected, marked alterations in subcortical tracts considered critical to seizure genesis. Our findings indicated that the type of white matter disruption (i.e., TW-AD) in combination with the disrupted region, may be relevant to the seizure semiology observed in FBTCS. Our results show that the region-specific alterations are likely a function of seizure pathology rather than whole-brain differences. The ensuing discussion focuses solely on the compelling results that could yield clinical utility; readers may refer to the Supplementary tables to further examine other results.

All patients versus controls As hypothesised, the whole-tract TW-ADC and TW-RD in several regions (ATR, CST, POPT, IFO, FPT, CC, STPOSTC, STPREC, STPREF, STPREM, TOCC, TPOSTC, TPREC, TPREF, TPREM) showed the familiar structural disruption described in focal epilepsy[15]. In focal epilepsy, increased ADC and RD suggests increased extracellular space and demyelination[35,36]. Further, animal models have shown that RD increases in white matter with demyelination, sometimes with unchanged AD[37]. Therefore, the TW-RD differences may reflect axonal damage due to seizures or, much less likely, indicate a promotor for seizure propagation through reduced inhibition. The significant differences in the ATR were notable and likely associated with seizure genesis due to many of our patients being diagnosed with frontotemporal epilepsy. The ATR has been used as a site for deep brain stimulation (DBS) to treat drug-refractory epilepsy [38,39]. The finding of altered ATR in our patient cohort offers further evidence that this tract could be a useful site for DBS treatment, however more research is required.

FBTCS-Y and FBTCS-N versus Controls One of the most remarkable findings was the significant difference (in TW-ADC, TW-AD) between the two patient subgroups in the IFO and STOCC and the TW-ADC of the TOCC tract. In patients with mesio-TLE, stereotactic EEG (SEEG) has shown the role of thalamocortical connections in seizure termination[40]. However, altered thalamic functional profiles have also been proposed as imaging biomarkers of active secondary generalisation[41]. Specifically, the thalamocortical circuit has been implicated as a critical mechanism for the genesis of FBTCS[42] by engagement of the striatum and CC.

The inhibitory role of the BG has been shown in TLE yet remains unclear in FBTCS. Mounting research using SEEG, DBS, and EEG/fMRI suggest the physiological rhythms in the BG as a "pacemaker" for ictal discharge throughout adjacent regions[10]. SEEG demonstrated cortico-striatal synchronisation[43], implicating the changing synchronisation as a mechanism to control the duration of abnormal oscillations within the striatal-thalamo-cortical loop and for potential termination. DBS studies show that regulation of BG activity via thalamostriatal projections may mediate generalised seizures[44]. Combined EEG/fMRI measurements showed the thalamocortical-striatal network could be involved in activation (thalamocortical), deactivation (striatal) and consequently termination of cortical discharge[45]. The cortico-striato-thalamo-cerebellar network has been implicated as a prominent feature of FBTCS via increased connectivity of structural covariance in the striatum and thalamus[50]. Here, we identified specific tracts (IFO, STOCC, TOCC) that may represent a predictive biomarker to differentiate between individuals who develop FBTCS versus those who do not. The increased TW-ADC in conjunction with the increased TW-AD could indicate white matter disruption significant enough to inhibit propagation of ictal discharge. This finding could guide researchers in investigating the specific circuits and networks involved in FBTCS.

The finding of a significant difference between the FBTCS-N and control groups in the TW-ADC, TW-FA and TW-RD of the TPREF and TPREM tracts might be explained by the gatekeeping function of the subcortical structures. The white matter disruption in those tracts may induce changes to their primary function in seizure activity, acting as a

protective mechanism that inhibits seizure propagation. Increased degradation of the fibre bundles that form the seizure propagation pathways may diminish the likelihood of ictal discharge traversing to the contralateral hemisphere. However, for those with less altered TPREF and TPREM tracts, such as in the FBTCS-Y group, the white matter fibre bundles may bear a closer resemblance to the control participants, thus the epileptogenic zone's ictal discharge could gain enough momentum to override the inhibitory mechanisms and cross to the contralateral hemisphere.

Alternatively, the white matter disruption in the FBTCS-N group may result from elevated BG activity during seizure inhibition. Extensive overworking of the pathways in the subcortical regions could manifest as axonal damage. In TLE, patterns of electrophysiological discharge propagation are purportedly bolstered by the structural white matter pathways, which reinforce ictal propagation[47], suggesting that white matter damage may halt the natural progression of ictal discharge.

Considering that the overall significant differences were observed between the FBTCS-N group and controls, the significantly higher TW-AD of the MCP in the FBTCS-Y group is noteworthy. Anatomically, the MCP crosses the two hemispheres, connecting the cerebellum to the pons, and is composed entirely of centripetal fibres, i.e., incoming fibres. Previous work has shown the role of the MCP in generalised tonic-clonic seizures[48], potentiating it as a tract whereby microstructural damage may impart susceptibility to the development of a generalised seizure.

Although increased AD has been shown to result from white matter maturation, all groups were age-matched, alluding to the possibility that the higher TW-AD in the MCP of the FBTCS-Y group may be due to distinct FBTCS mechanisms. Since increased AD can also imply better organisation of fibre structure, the TW-AD differences between the FBTCS-Y and FBTCS-N groups in the cerebellar region could be a feature of the FBTCS brain whereby those with FBTCS-Y have better fibre connections and the ability to sustain the intrahemispheric flow of ictal discharge. Conversely, our FBTCS-N group may have more damaged or poor fibre connections, evidenced by the overall higher TW-ADC and TW-RD in the thalamus, striatal and CC tracts compared to the FBTCS-Y and control groups. Lastly, though the ICP is anatomically adjacent to the SCP and MCP, it is not

functionally important in inhibition nor information relay, which may explain its non-significance in both group comparisons, and underscore the potential functional importance of the MCP in FBTCS. Our findings promote the possibility that propagation of ictal discharge from the epileptogenic zone to the contralateral hemisphere could be inhibited by damage to critical information relay and anatomically relevant tracts.

Interestingly, SEEG work has presented a paradoxical phenomenon of concurrent, increased structural connectivity in the epileptogenic zone and propagation zone, and decreased widespread connectivity suggests that distributed functional networks may be disintegrated, while epileptic networks are spared[49]. Though such disintegrated functional networks may not be implicated explicitly in focal epilepsy, their presence may play a role in seizure inhibition when seizures shift from focal to tonic-clonic. This may explain why overall, the TW-TMs of the FBTCS-N group indicated increased white matter disruption, yet in contrast, patients with FBTCS appeared more congruent to healthy controls. Finally, there was no significant relationship between lesion presence and seizure onset side, or lesion presence and FBTCS, reinforcing the prospect that the region-specific differences between the patient subgroups were due to premorbid connections rather than the effects of injury.

Imaging studies of patients with epilepsy are traditionally limited by small sample sizes[17,18,19,50], primarily due to challenges in recruitment. Our relatively small sample size was a limitation in our study, which prevented further analysis of the striatal and thalamus regions. Nevertheless, our study emphasises that specific tracts may play a role in FBTCS, reinforcing the value of structural imaging in demystifying the mechanisms involved in FBTCS. Though generalised seizures may appear semiologically similar to FBTCS, specific pathways and networks may be involved in FBTCS once the bi-hemispheric ictal propagation begins and is an essential subject for further research.

In summary, we used advanced diffusion imaging techniques to show region-specific microstructural alterations in patients with and without FBTCS, compared to control participants. Our findings provide mechanistic insights into the potential impact of structural changes on the functional role of the thalamic and striatal regions in focal epilepsy and its FBTCS subtype. We highlight specific tracts that may be involved in

inhibition (IFO, STOCC) or promotion (MCP), of FBTCS. Our results add to current knowledge of seizure propagation in FBCTS, and offer potential biomarkers that can help explain disease progression and aid treatment.

5 ACKNOWLEDGEMENTS

The authors would like to acknowledge all staff at the Comprehensive Epilepsy Centre at the RPAH, particularly Mrs Maricar Senturias (RN/ACNC Epilepsy), who assisted with patient recruitment. The authors would like to acknowledge the radiology staff at I-MED Radiology for their assistance with obtaining the MRI data. All authors would like to acknowledge the research funding support from UCB Australia Pty Ltd.

CM would like to acknowledge scholarship support from the Nerve Research Foundation, University of Sydney. AD acknowledges funding from St. Vincent's Hospital. OK acknowledges the partial support provided by The University of Sydney through a SOAR Fellowship and Microsoft's partial support through a Microsoft AI for Accessibility grant. CW acknowledges research funding from the Nerve Research Foundation, University of Sydney.

6 CONFLICTS OF INTEREST

None of the authors has any conflicts of interest to disclose.

7 ETHICAL PUBLICATION STATEMENT

We confirm that we have read the Journal's position on issues involved in ethical publication and affirm that this report is consistent with those guidelines.

References

1. Park KJ, Sharma G, Kennedy JD, Seyal M. Potentially high-risk cardiac arrhythmias with focal to bilateral tonic–clonic seizures and generalized tonic–clonic seizures are associated with the duration of periictal hypoxemia. Epilepsia. 2017;58:2164–71.
2. Lawn ND, Bamlet W, Radhakrishnan K, O'Brien P, So EL. Injuries due to seizures in persons with epilepsy: a population-based study. Neurology. 2004;63:1565–70.
3. Sveinsson O, Andersson T, Carlsson S, Tomson T. The incidence of SUDEP: a nationwide population-based cohort study. Neurology. 2017;89:170–7.

4. Blumenfeld H, Westerveld M, Ostroff RB, et al. Selective frontal, parietal, and temporal networks in generalized seizures. Neuroimage. 2003;19:1556–66.
5. Schindler K, Leung H, Lehnertz K, Elger CE. How generalised are secondarily "generalised" tonic–clonic seizures?. J Neurol Neurosurg Psychiatry. 2007;78:993–6.
6. Hwang K, Bertolero MA, Liu WB, D'Esposito M. The human thalamus is an integrative hub for functional brain networks. JNeurosci. 2017;37:5594–5607.
7. Norden AD, Blumenfeld H. The role of subcortical structures in human epilepsy. Epilepsy & Behav. 2002;3:219–31.
8. Blumenfeld H. The thalamus and seizures. Arch Neurol. 2002;59:135–7.
9. Smith Y, Bevan M, Shink E, Bolam JP. Microcircuitry of the direct and indirect pathways of the basal ganglia.. Neuroscience.1998;86:353–87.
10. Rektor I, Kuba R, Brázdil M, Chrastina J. Do the basal ganglia inhibit seizure activity in temporal lobe epilepsy?. Epilepsy Behav. 2012;25:56–59.
11. Feddersen B, Remi J, Kilian M, et al. Is ictal dystonia associated with an inhibitory effect on seizure propagation in focal epilepsies?. Epilepsy Res. 2012;99:274–80.
12. Uchida CGP, Barsottini OGP, Caboclo LOSF, et al. Does the patient's hand hold the key to preventing secondary generalization in mesial temporal lobe epilepsy?. Epilepsy Res 2013;105:125–32.
13. Rektor I, Kuba R, Brázdil M. Interictal and ictal EEG activity in the basal ganglia: an SEEG study in patients with temporallobe epilepsy. Epilepsia. 2002;43:253–62.
14. Pizzo F, Roehri N, Giusiano B, et al. The ictal signature of thalamus and basal ganglia in focal epilepsy: a SEEG study. Neurology. 2021;96:e280–93.
15. Hatton SN, Huynh KH, Bonilha L, et al. White matter abnormalities across different epilepsy syndromes in adults: an ENIGMA-Epilepsy study. Brain. 2020;143:2454–73.
16. Slinger G, Sinke MR, Braun KP, Otte WM. White matter abnormalities at a regional and voxel level in focal and generalized epilepsy: a systematic review and meta-analysis. Neuroimage Clin. 2016;12:902-09.
17. Chiang S, Levin HS, Wilde E, Haneef Z. White matter structural connectivity changes correlate with epilepsy duration intemporal lobe epilepsy. Epilepsy Res. 2016;120:37–46.

18. Lemkaddem A, Daducci A, Kunz N, et al. Connectivity and tissue microstructural alterations in right and left temporal lobeepilepsy revealed by diffusion spectrum imaging. Neuroimage Clin. 2014;5:349–58.
19. Sone D, Sato N, Kimura Y, Watanabe Y, Okazaki M, Matsuda H. Brain morphological and microstructural features incryptogenic late-onset temporal lobe epilepsy: a structural and diffusion MRI study. Neuroradiology. 2018;60:635–41.
20. Andersson JL, Sotiropoulos SN. An integrated approach to correction for off-resonance effects and subject movement indiffusion MR imaging. Neuroimage 2016;125:1063–78.
21. Fischl B. FreeSurfer. Neuroimage. 2012 15;62:774-81
22. Tournier JD, Smith R, Raffelt D, et al. MRtrix3: A fast, flexible and open software framework for medical image processing and visualisation. Neuroimage. 2019;202:116137.
23. Smith SM, Jenkinson M, Woolrich MW, et al. Advances in functional and structural MR image analysis and implementationas FSL. Neuroimage. 2004;23:S208–19.
24. Tustison NJ, Avants BB, Cook PA, et al. N4ITK: improved N3 bias correction. IEEE Trans Med Imaging 2010;29:1310–20.
25. Dhollander T, Raffelt D, Connelly A. Unsupervised 3-tissue response function estimation from single-shell or multi-shell diffusion MR data without a co-registered T1 image. In ISMRM Workshop on Breaking the Barriers of Diffusion MRI. 2016;5.
26. Smith RE, Tournier JD, Calamante F, Connelly A. Anatomically-constrained tractography: improved diffusion MRIstreamlines tractography through effective use of anatomical information. Neuroimage. 2012;62:1924–38.
27. Tournier JD, Calamante F, Connelly A. Improved probabilistic streamlines tractography by 2nd order integration over fibre orientation distributions. In Proceedings of the international society for magnetic resonance in medicine. 2010;1670. New Jersey, USA: John Wiley & Sons, Inc..
28. Smith RE, Tournier JD, Calamante F, Connelly A. SIFT2: Enabling dense quantitative assessment of brain white matterconnectivity using streamlines tractography. Neuroimage. 2015;119:338–51.

29. Calamante F, Tournier JD, Jackson GD, Connelly A. Track-density imaging (TDI): super-resolution white matter imagingusing whole-brain track-density mapping. Neuroimage. 2010;53:1233–43.
30. Alexander AL, Lee JE, Lazar M, Field AS. Diffusion tensor imaging of the brain. Neurotherapeutics. 2007;4:316–29.
31. Calamante F. Track-weighted imaging methods: extracting information from a streamlines tractogram. Magn Reson Mater Phy. 2017;30:317–35.
32. Willats L, Raffelt D, Smith RE, Tournier JD, Connelly A, Calamante F. Quantification of track-weighted imaging (TWI):characterisation of within-subject reproducibility and between-subject variability. Neuroimage. 2014;87:18–31.
33. Wasserthal J, Neher P, Maier-Hein KH. TractSeg-Fast and accurate white matter tract segmentation. Neuroimage. 2018;183:239–53.
34. Lebel C, Gee M, Camicioli R, Wieler M, Martin W, Beaulieu C. Diffusion tensor imaging of white matter tract evolutionover the lifespan. Neuroimage. 2012; 60:340–52.
35. Arfanakis K, Hermann BP, Rogers BP, Carew JD, Seidenberg M, Meyerand ME. Diffusion tensor MRI in temporal lobe epilepsy. Magn Reson Imaging. 2002;20:511-9.
36. Concha L, Beaulieu C, Collins DL, Gross DW. White-matter diffusion abnormalities in temporal-lobe epilepsy with and without mesial temporal sclerosis. J Neurol Neurosurg Psychiatry. 2009;80:312-9.
37. Song SK, Sun SW, Ramsbottom MJ, Chang C, Russell J, Cross AH. Dysmyelination revealed through MRI as increased radial (but unchanged axial) diffusion of water. Neuroimage. 2002;17:1429-36.
38. Hodaie M, Wennberg RA, Dostrovsky JO, Lozano AM. Chronic anterior thalamus stimulation for intractable epilepsy. Epilepsia. 2002;43:603–08.
39. Lehtimäki K, Möttönen T, Järventausta K, et al. Outcome based definition of the anterior thalamic deep brain stimulation target in refractory epilepsy. Brain Stimul. 2016;9:268–75.
40. Evangelista E, Bénar C, Bonini F, et al. Does the thalamo-cortical synchrony play a role in seizure termination?. Front Neurol. 2015;6:92.

41. Caciagli L, Allen LA, He X, et al. Thalamus and focal to bilateral seizures: A multiscale cognitive imaging study. Neurology. 2020;95:e2427–41.
42. Brodovskaya A, Kapur J. Circuits generating secondarily generalized seizures. Epilepsy Behav. 2019;101:106474.
43. Aupy J, Wendling F, Taylor K, Bulacio J, Gonzalez-Martinez J, Chauvel P. Cortico-striatal synchronization in human focal seizures. Brain. 2019;142:1282–95.
44. Velasco AL, Velasco F, Jiménez F, et al. Neuromodulation of the centromedian thalamic nuclei in the treatment of general- ized seizures and the improvement of the quality of life in patients with Lennox–Gastaut syndrome. Epilepsia. 2006;47:1203–12.
45. Moeller F, Siebner HR, Wolff S, et al. Changes in activity of striato–thalamo–cortical network precede generalized spike wave discharges. Neuroimage. 2008;39:1839–49.
46. Xu Q, Zhang Q, Yang F, et al. Cortico-striato-thalamo-cerebellar networks of structural covariance underlying different epilepsy syndromes associated with generalized tonic–clonic seizures. Hum Brain Mapp. 2021;42:1102–15.
47. Gleichgerrcht E, Greenblatt AS, Kellermann TS, et al. Patterns of seizure spread in temporal lobe epilepsy are associated with distinct white matter tracts. Epilepsy Res. 2021;171:106571.
48. Jiang S, Li X, Li Z, et al. Cerebello-cerebral connectivity in idiopathic generalized epilepsy. Eur Radiol. 2020;30:3924–33.
49. Besson P, Bandt SK, Proix T, et al. Anatomic consistencies across epilepsies: a stereotactic-EEG informed high-resolution structural connectivity study. Brain. 2017;140:2639–52.
50. Liu M, Chen Z, Beaulieu C, Gross DW. Disrupted anatomic white matter network in left mesial temporal lobe epilepsy. Epilepsia. 2014;55:674–82.